https://doi.org/10.5194/egusphere-2023-1907
Preprint. Discussion started: 30 August 2023

Regional analysis of convective heavy rain events in the German State of Hesse

Manuel Perschke[1,2], Britta Schmalz[1], Ernesto Ruiz Rodriguez[2]

[1]Chair of Engineering Hydrology and Water Management, Technical University of Darmstadt, Darmstadt, 64289, Germany
[2]Chair of Hydraulic Engineering and Water Management, RheinMain University of Applied Sciences, Wiesbaden, 65197, Germany

Correspondence to: Manuel Perschke (manuel.perschke@hs-rm.de)

Abstract. The convective heavy precipitation events, which occur primarily in the summer months, cannot be recorded representatively by ground-based precipitation stations due to their frequently small spatial extent, short life span and high rapidly changing intensity. The radar network of the German Weather Service, on the other hand, records area-wide, spatiotemporally highly resolved precipitation information that enables comprehensive identification of precipitation objects. In this study, a method for the identification, description and classification of convective precipitation objects considering a flood-relevant event extent is presented. Assuming an orographic independence of the events in the Central European low mountain range, the German State of Hesse is chosen as representative study area. Considering the spatial and temporal extent of the identified events, the most extreme expression is selected and independence is ensured. With the assignment of an authoritative duration for the intensive main rainfall phase, an extensive collection of heavy precipitation objects results. The results show a characteristic event length of 15 to 60 minutes; longer durations are underrepresented and exhibit inhomogeneous extreme value behavior. Statistically, the generated samples can be well represented and classified by the generalized extreme value distribution. The evaluation allows us to make a regional characterization of convective heavy precipitation.

https://doi.org/10.5194/egusphere-2023-1907
Preprint. Discussion started: 30 August 2023

1 Introduction

When considering the development of heavy precipitation events, a distinction must be made between stratiform and convective precipitation events. With increasing duration of heavy rain events, we assume a decrease in precipitation intensity or intensity peaks. Due to the different change behavior from the precipitation type and depending on the prevailing duration stage, a differentiated consideration of the events should be made. Summer heavy rainfall events are largely represented by thermal-induced convective precipitation. Convective precipitation events show a high spatial and temporal variability. They are generally characterized by a small precipitation field (< 100 km²) with limited vertical extension and high and rapidly changing intensities.

With continuing global warming, the question of the changing behavior of heavy precipitation in Germany respectively the temperate climate zone of Central Europe is becoming increasingly important, as reflected in the latest IPCC (Bednar-Friedl et al., 2022) and German KLIWA report (Müller et al., 2019). From a physical point of view, an increase in the depth of precipitation as well as intensification on a convective level can be expected due to the increased water vapor capacity of the atmosphere. This effect is determined as the Clausius-Clapeyron (CC) relationship, which gives an increase in specific saturation moisture of about 7 % per degree of heating. In examining the temperature dependence of different forms of precipitation, Berg and Haerter (2013) found that stratiform events did not exhibit a pronounced temperature dependence and, conversely, convective events had an increase in intensity above the CC relationship. In this context Lenderink et al. (2017) find a twice CC relation (2CC – Super Clausius-Clapeyron) when examining the large-scale atmospheric condition in summer precipitation events in the Netherlands, which they interpret as a response of extreme precipitation to climate change. The analysis of the historical and future behavior of summer precipitation using convection-permitting models (CPM) shows an increase in hourly precipitation extremes with a constant number of convective cells (Knist et al., 2018; Purr et al., 2021). The change is strongest in the range of the most extreme events, resulting in an increase of larger intense precipitation cells.

Considering these projections, an increased risk of heavy rainfall-initiated flash floods in smaller catchment areas is to be expected in the European low mountain ranges. In terms of flood prevention, it is necessary to identify potentially vulnerable areas and to simulate the consequences of extreme heavy rainfall events with the assistance of hydraulic rainfall-runoff models. For a long time, it was common in Germany to use station-based statistical model rainfall as input for such simulations. In some German states, the use of exceptional scenarios (Baden-Wuerttemberg) or historical radar-based events (Hesse) has become established in the field of heavy rainfall risk management in recent years. Especially for hourly and smaller precipitation extremes, the representation quality by ground-based precipitation stations is insufficient. Due to their small spatial extent and short-lived nature, convective events are not recorded by these stations, or only at specific points (Purr et al., 2018). This stationary recording is not representative for the track or the entire life span of a convective cell. At this point the necessity of area-wide, high-resolution radar precipitation data for the quantitative detection of convective events becomes apparent. It should be mentioned that the qualitative accuracy of the precipitation data results from the combination

https://doi.org/10.5194/egusphere-2023-1907
Preprint. Discussion started: 30 August 2023

of both data acquisition methods: punctual measurement and area-wide estimation. The result are nationwide calibrated radar products from the German Weather Service (DWD) – RADOLAN and RADKLIM.

A statistical analysis based on hourly radar precipitation totals (RADKLIM-RW Version 2017.002) was performed as part of the RADKLIM project (Winterrath et al., 2017) for durations between 1 and 72 hours. For the individual grid cells of the DWD radar network (nationwide), partial series of the highest-rated precipitation events are formed. The calculation approach is derived from DWA worksheet 531 (Haberlandt et al., 2017) and used an exponential distribution to determine the quantiles. Winterrath et al. (2017) noted that for short duration stages and large recurrence interval T (> 20 a), the distribution of statistical precipitation was inhomogeneous and less related to relief. In this case, the strong inhomogeneity could be attributed to the short observation period and the single occurrence of local extreme events.

The aim of this study is to develop a methodological approach for the identification, characterization and evaluation of short intense heavy precipitation events. In this approach, common procedures of precipitation statistics are taken up and adapted to the spatial and temporal characteristics of convective precipitation objects. As a necessary data basis, the climatologically processed 5-min precipitation data (RADKLIM-YW Version 2017.002) from the radar network of the DWD are used.

2 Methodology

2.1 Data processing

The DWD provides the YW data in binary, netCDF and ascii raster format on their server service. For more efficient processing, the entire dataset was converted to GeoTIFF format within the framework of this study. In this way, the storage requirement can be reduced to 100 GB (unpacked) and the access speed can be increased many times over. For this purpose, the binary data were transformed into a matrix and assigned a precipitation value (between 0 and 4095) or no-data value according to the 13th-16th bit coding. In order to reduce the memory requirement, the decimal point representation is omitted - as with the input data - and a 16-bit integer format is selected. For the representation of the precipitation values in mm, the data must be multiplied by 0.01 during processing. In addition to the low storage requirements, the data are geo-referenced in GeoTIFF format and can be easily adapted to the study area and period. The data have a spatial resolution of 1 km² and are currently available for the period between 2001 and 2021 – they are updated every year. A detailed intercomparison of national radar products and station data from the DWD was implemented by Kreklow et al. (2019).

For further processing of the radar precipitation data, the time series generated for the separate grid cells cover the entire observation period. The pilot study is carried out on the example of the German State of Hesse with an approx. area of 25000 raster cells. The state has a double spatial coverage by the DWD radar network with the exception of two sub-areas in the south and north (Fig. 2a). The temporal continuity of the radar record is largely given. The exception is a sub-area in the north of Hesse, where a data gap occurred in the hydrological summer of 2014 due to a conversion of the Flechtdorf radar site.

https://doi.org/10.5194/egusphere-2023-1907
Preprint. Discussion started: 30 August 2023

2.2 Previous studies

In the context of this pre-study, the suitability of the input data for the overall study objective is examined. This concerns on the one hand the mapping quality of the RADKLIM data for the detection of convective precipitation objects and on the other hand the representativeness and orographic independence of the selected study area. The location of the study area Hesse, is shown in Fig. 1 and is part of the Central European low mountain sill. The natural area extends from the Ardennes (Belgium) in the west to the Bohemian Massif (Czech Republic) in the east, covering a large part of Germany between the northern lowlands as well as the foothills of the Alps and the Black Forest in the south. Hesse forms a representative section in the center of this natural area.

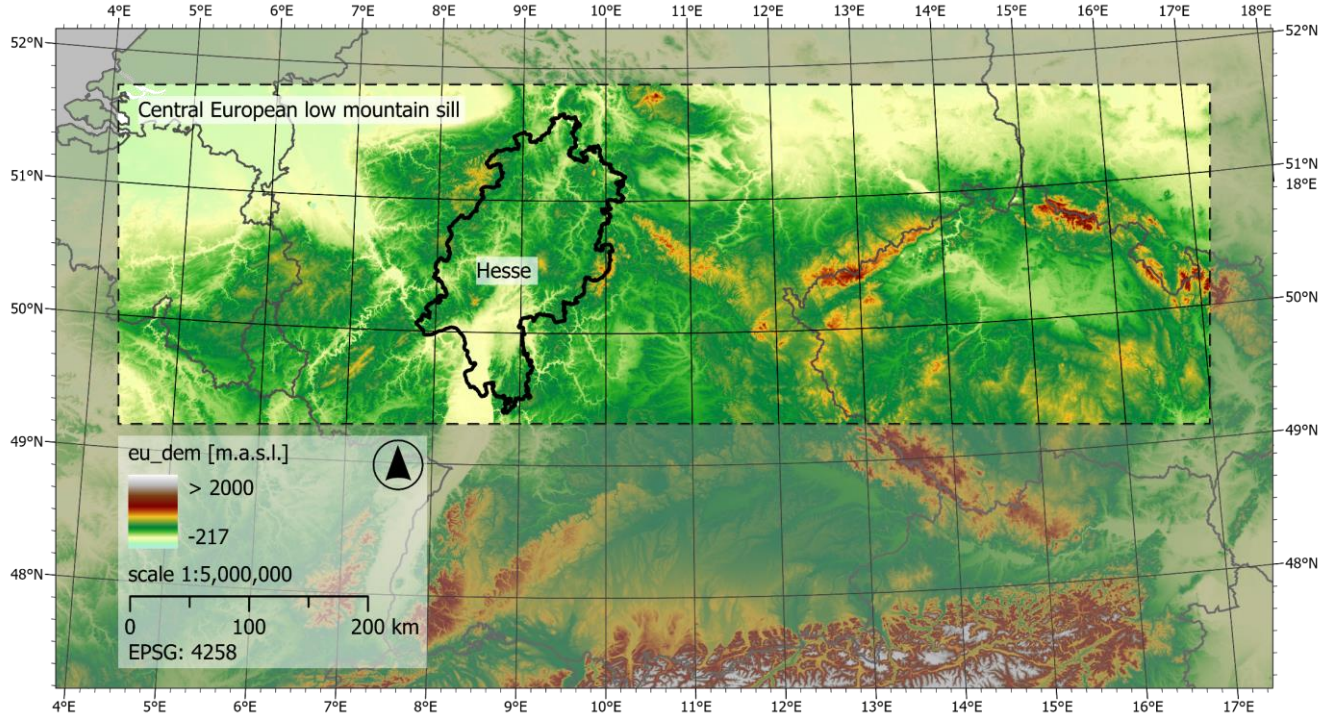

Figure 1: Location of Hesse in the Central European low mountain sill. Base map: EU-DEM v1.1 [CLMS]

2.2.1 Event catalogue

In addition to the statistical analysis of hourly radar precipitation totals, the DWD has compiled a heavy rainfall catalog based on the same data (Lengfeld et al., 2022). The Catalogue of Radar-based heavy Rainfall Events (CatRaRE) contains a collection of spatially and temporally independent precipitation objects of distinguished duration stages (1-72 h), which are statistically defined as heavy rains. An evaluation of the one-hour heavy rainfall objects shows a characteristic event extent of 9 (minimum) to approximately 100 grid cells when considering the 95% percentile. The determination of the statistical parameters of the data set resulted in a modal value of 9 and an arithmetic mean value of 25 grid cells. The values show the characteristic extent of short and spatially limited heavy precipitation events. For the selected data, the potential coverage of precipitation objects

https://doi.org/10.5194/egusphere-2023-1907
Preprint. Discussion started: 30 August 2023

by high-resolution ground-based precipitation stations was evaluated over the area of Hesse. For this purpose, a spatial intersection of station locations and precipitation fields was performed. In total, 82 stations of the DWD and 40 stations of the Hessian Agency for Nature Conservation, Environment and Geology (HLNUG) are available in Hesse. It is shown that only about 10 percent of the events could be recorded by the stations, neither the temporal coverage, the spatial distribution and the intensity focus nor possible station failures at the time of the event are taken into account.

2.2.2 Orographic independence

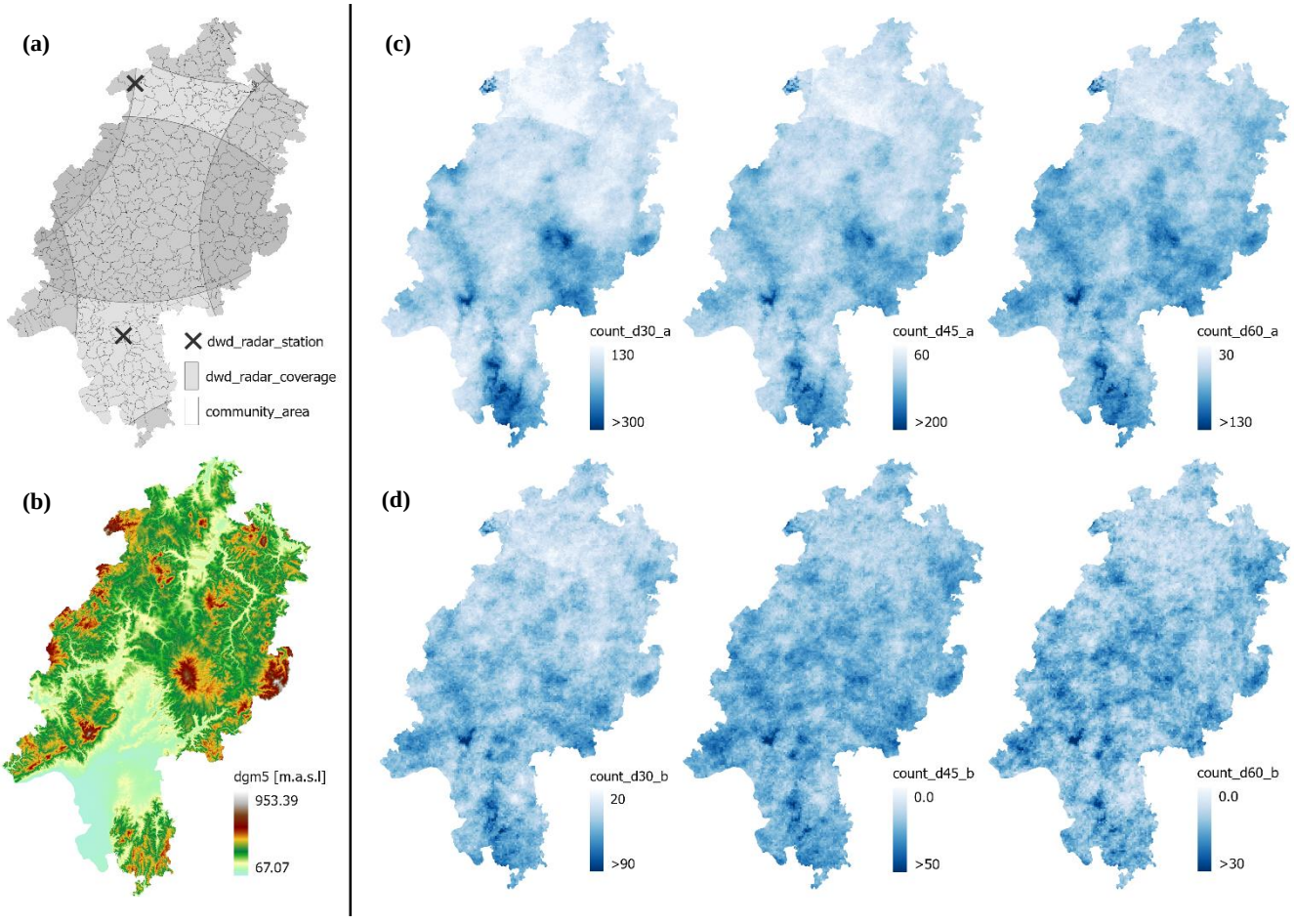

Figure 2: Count of independent convective events in Hesse between 2001 and 2021 (hydrological summer) for different durations (30, 45, 60 min) and different thresholds 8.5 mm/h (c) and 15.0 mm/h (d). Base maps (left): German radar network [DWD] (a), digital elevation model 5 [HVBG] (b).

Topographically, the region is characterized in the south by the Rhine-Main plain and in the central and northern parts by the German low-mountain sill (Fig. 2b). Here the question arises what influence the orography has on the convection potential in Hesse. Kirshbaum et al. (2018) describe the various orography-related mechanisms to initiated convection. This shows that potentially convection occurs more frequently at higher altitude.

https://doi.org/10.5194/egusphere-2023-1907
Preprint. Discussion started: 30 August 2023

Figure 2c shows the number of independent convective events for the 30 min, 45 min and 60 min duration periods in the hydrologic summer half-year (May, June, July, August, September and October) between 2001 and 2021 at a threshold of 8.5 mm/h - which was defined for convective cells in other publications (e. g. Brendel et al., 2014). It can be seen that for short events (≤ 45 min) there is a clear dependence on orography - the largest number of events is recorded in the area of the higher low mountain ranges. With increasing duration (≥ 60 min) the occurrence maxima become detached from the orography. The comparatively low values in northern Hesse are due to the conversion of the Flechtdorf radar. In this zone, there is only single radar coverage – compare Fig. 2a. The same analysis was performed in Fig. 2d with a threshold value of 15 mm/h, which is set for the identification of heavy precipitation events. The distribution of the occurrence rate over Hesse is more homogeneous and orographically decoupled. This supports the assumption that low mountain ranges initiate a higher number of convective events, but not necessarily a high intensity. Purr et al. (2018) explain this effect by the fact that the capping inversion at the upper edge of the boundary layer is more easily interrupted in the mountains than in the lowlands, so that instability can build up for a longer time in the lowlands before enhanced high-range convection is induced. Due to orography-related mechanisms, convective precipitation cells are often in the initial stage, which may imply lower intensity.

2.3 Main approach

Taking into account the results of previous evaluations (Sect. 2.2), the aim of this study is to optimize the methodology for the statistical evaluation of short intense heavy precipitation events. The method is adapted to the spatial and temporal characteristics of the sample of convective precipitation objects. The approach includes identification of independent convective precipitation objects, the formation of a spatiotemporally representative sample and the application of an appropriate distribution function to determine the quantiles of the extreme events. With the help of the spatial aggregation of the radar precipitation data, the disturbing influence of inhomogeneities – as described in the introduction – on the statistical analysis can be reduced. By averaging the single values over a defined cell cluster, the relation to the characteristic expansion of convective events is taken.

2.3.1 Identification of extreme events

To adapt the sample to the characteristics of convective precipitation events, several evaluation steps have to be performed. The evaluation is based on the generated time series of the single grid cells (Sect. 2.1). The analysis is performed according to the scheme in Fig. 3 and is divided into four automated processing steps. The first two process steps are applied to all grid cells, while steps three and four are scaled to the entire study area.

https://doi.org/10.5194/egusphere-2023-1907
Preprint. Discussion started: 30 August 2023

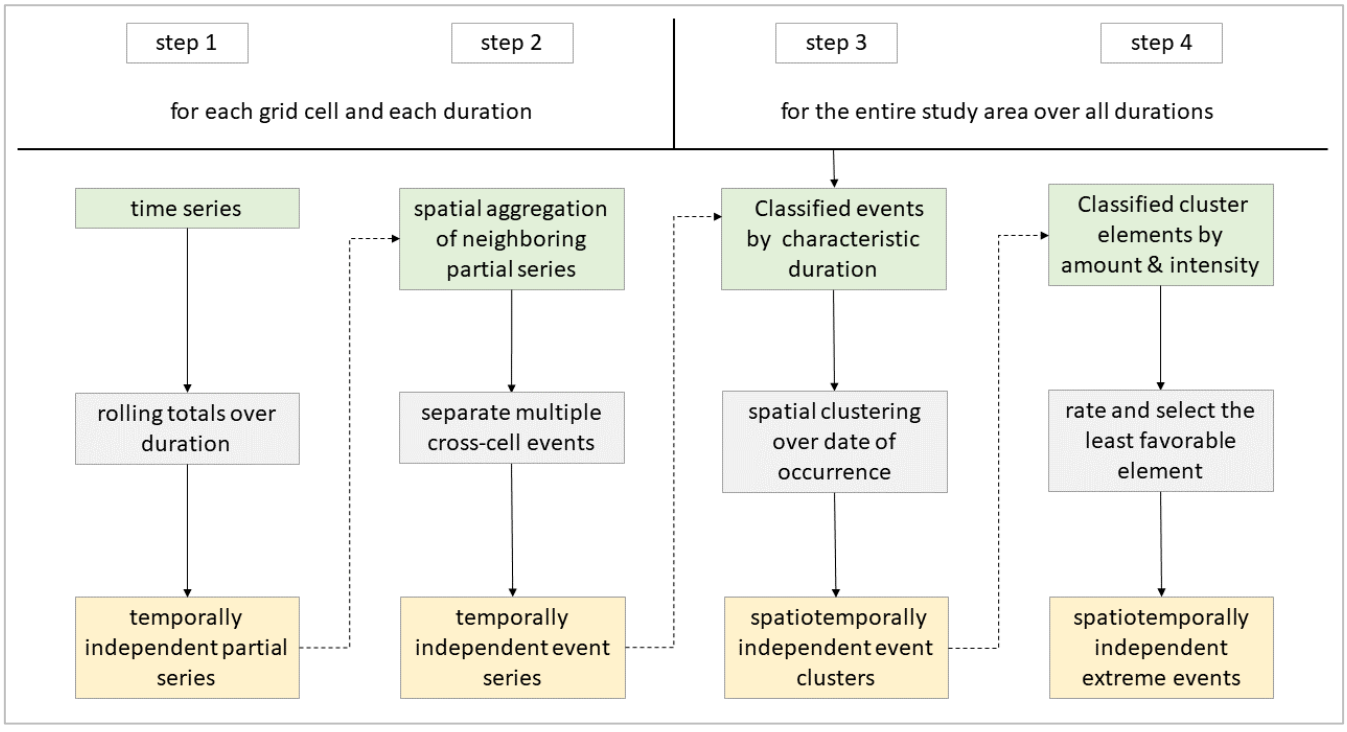

Figure 3: Evaluation scheme for the identification and characterization of spatiotemporally independent extreme events. Green: pre-processed input, grey: evaluation step and yellow: (interim) output.

Step 1 – Partial series

In the first step, the temporal aggregation of the precipitation data is carried out according to the procedure from DWA Worksheet 531 (Haberlandt et al., 2017). Rolling totals (partial sum) are formed for a specific set of precipitation durations d between 15 and 90 minutes with a 15-minute interval. The maxima are selected from the resulting aggregations (e.g., Table 1a) and independence is ensured by a precipitation-free interval of at least four hours between each local maximum. The number of temporal independent maxima per grid cell is limited to the 1000 highest values for the partial series.

Step 2 – Spatial aggregation

With spatial aggregation, a cross-cell intersection of precipitation events for each individual cell in the study area is performed in this step. For this purpose, the partial series of the target cell and its neighboring cells are merged and the identified local maxima are evaluated. According to the characteristic extent of convective precipitation events (Sect. 2.2.1), the first order neighbors (3 X 3 grid cells) and the second order neighbors (5 X 5 grid cells) are considered. In the evaluation process, the partial series are contrasted and those local maxima are filtered out which occur in a given time period both in the target cell and in all 8 or 24 neighboring cells. To ensure that they are the same precipitation event, the maximum temporal distance Δt between the neighboring maxima of the grid cells is set to the interval of the considered precipitation duration d. If both criteria are met, the mean value of the local maxima is calculated and included in the event series of the target cell.

https://doi.org/10.5194/egusphere-2023-1907
Preprint. Discussion started: 30 August 2023

Table 1: Evaluation scheme for the definition of extreme precipitation events of a single grid cell 580828 on the example of a first-order neighbor aggregation and a specific duration of 45 minutes.

a) Identification of local maxima of precipitation totals [mm] (bold) from a series of rolling totals over 45 minutes for target cell 645/327 and first-order neighboring cells. The time stamp of the local maxima indicates the starting point of aggregation.

time stamp	644/326	644/327	644/328	645/326	**645/327**	645/328	646/326	646/327	646/328
…	…	…	…	…	…	…	…	…	…
31.05.2003 12:20	96.21	95.26	33.59	68.34	53.23	43.80	45.28	49.57	43.98
31.05.2003 12:25	104.98	105.44	44.87	73.83	56.03	77.22	50.81	55.77	56.72
31.05.2003 12:30	**106.26**	**107.35**	**45.39**	88.56	**69.80**	**90.54**	61.51	71.36	59.94
31.05.2003 12:35	106.00	106.75	45.39	**88.77**	69.60	90.48	**62.11**	**71.73**	**64.6**
31.05.2003 12:40	101.08	102.52	44.99	82.37	65.15	90.21	58.98	65.30	63.09
31.05.2003 12:45	94.58	101.21	42.72	74.20	59.07	88.25	54.83	58.51	61.30
31.05.2003 12:50	73.58	78.02	27.05	62.22	49.52	71.91	49.16	51.55	46.47
31.05.2003 12:55	54.97	46.16	24.04	44.2	43.56	63.51	41.13	46.2	39.64
31.05.2003 13:00	45.84	37.88	17.33	41.56	42.22	55.92	37.45	44.75	30.97
31.05.2003 13:05	16.42	15.85	13.35	25.99	20.1	48.78	20.82	26.74	21.73
31.05.2003 13:10	7.68	5.71	2.12	20.52	17.31	15.40	15.30	21.03	9.37
…	…	…	…	…	…	…	…	…	…

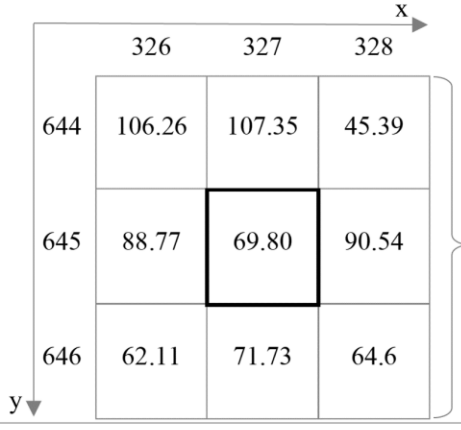

b, left) Raster location (RADKLIM) of target cell and the first-order neighbors with their related local maxima.

c, right) Temporally independent event series of the target cell for a duration of 45 minutes. The mean value is formed from the related local maxima.

time stamp start	d	mean	max	original	r_id	y	x
31.05.2003 12:30	**45**	**78.51**	**107.35**	**69.8**	**580828**	**645**	**327**
07.08.2004 16:20	45	32.25	48.7	33.23	580828	645	327
14.08.2020 11:55	45	31.85	49.86	27.49	580828	645	327
…	…	…	…	…	…	…	…

Table 1 shows the evaluation scheme for the definition of extreme events of a single gride cell. As an example, the evaluation of a precipitation event of duration 45 minutes is performed for grid cell 580828 with RADKLIM coordinates y = 645 and x = 327. The first-order neighbors are considered. This method aims to derive from radar data a kind of area precipitation for specific event extents and to reduce the influence of extreme single values - potential outliers or false values - of a precipitation cluster. By averaging the neighboring local precipitation maxima (e.g., Table 1b), the most extreme expression of a cross-cell event is considered. Spatial smoothing of the input radar data is not performed here due to the temporal shift between local maxima of precipitation totals over the course of an event. The result is a temporally independent event series for each grid cell (e.g., Table 1c).

https://doi.org/10.5194/egusphere-2023-1907
Preprint. Discussion started: 30 August 2023

Step 3 – Characteristic duration and event clustering

The generated data series of the single grid cells contain elements that represent the same event over different precipitation durations. In this step, one characteristic duration – 15, 30, 45, 60, 75 or 90 min – is assigned to each event. As a condition for the assignment, a relative change of at least 10 % from the initial value per 15 min and an absolute change of 5 mm per 15 min to the next higher duration is defined. The highest duration that fits this condition is considered decisive. This ensures a sufficient intensity of the extreme event with increasing duration. Table 2 shows the selection for a single event of the grid cell 580828, the event is classified by a duration of 45 minutes. For each grid cell, a series of uniquely classified elements is generated.

Table 2: Assignment of a characteristic duration to a single event in grid cell 580828. Selection thresholds is 10 % relative and 5 mm absolute change from the previous precipitation depth. The selected duration is bold.

duration [min]	time stamp start	depth [mm]	absolut change [mm]	relativ change [%]
15	2003-05-31 12:40	43.6	-	-
30	2003-05-31 12:40	69.76	26.16	60.00
45	**2003-05-31 12:30**	**78.51**	**8.75**	**12.54**
60	2003-05-31 12:25	79.84	1.33	1.69
75	2003-05-31 12:25	81.26	1.42	1.78
90	2003-05-31 12:25	82.24	0.98	1.21

Subsequently, the evaluation is scaled to the entire study area. All classified event series – over all specified durations – are merged and the elements grouped according to their date of occurrence. The date-grouped elements are plotted into the RADKLIM grid using their local coordinates (y, x); all surrounding cells are classified as NaN. The spatial relation of the gridded single elements is established by the formation of event clusters. The Clustering is done by a region labeling (connected-component), which splits the input raster into multiple numbered segments. The selected 8-way connectivity captures the square and diamond neighborhood of the cells. The spatiotemporally independent event clusters are defined by selecting key areas (segments) with an area of at least 9 grid cells. Smaller event zones are not considered.

Step 4 – Event classification

In the last evaluation step, the least favorable expression over the entire spatial and temporal extent is defined for each identified event cluster. For this purpose, the individual cluster elements are ranked according to their precipitation depth and intensity. The sum of both criteria ranks is formed and the highest ranked element is selected. It is not established that the largest depth of precipitation and often longer duration simultaneously defines the most extreme expression. The goal is not to identify and classify the entire event with pre and post rain, but the main intense period. The selected elements are again grouped according to their duration and stored as a data set for further processing. The precipitation objects are described in the resulting dataset by several attributes, such as timestamp, mean precipitation depth and intensity, grid id, coordinates (EPSG 25832), etc.

https://doi.org/10.5194/egusphere-2023-1907
Preprint. Discussion started: 30 August 2023

Representative sample

In the previous chapters, the statistical robustness of the recording period and the number of spatially bounded convective heavy precipitation events have already been discussed. For further analysis of the identified extreme precipitation objects (resulting data set), a seasonal representative subset must be defined. A combination of two selection methods is used: peak over threshold (POT) and block-maxima (BM). Via a fixed threshold value (POT) per duration – shown in Table 3 – the events are checked and selected on their extremity. The values are oriented to the general warning criteria for heavy rainfall of the DWD and are assumed to be representative for the Central European low mountain ranges.

Table 3: Precipitation intensity threshold per duration for the definition of extreme events. Oriented to the DWD's warning criteria for heavy precipitation.

duration [min]	15	30	45	60	75	90
intensity [mm/h]	30	25	20		15	

For the BM method, a non-overlapping monthly interval in the hydrological summer season – May till October – is selected and the corresponding highest precipitation objects are separated. It is not guaranteed that for every year and every month an extreme event can be identified. In this approach, annual and seasonal variations in the observation period are consistently taken into account. The aim is to avoid that the influence of extreme years or months takes an over-representative part of the data collective. The resulting subsets (samples) over the entire area for each characteristic duration and spatial aggregation are subjected to statistical evaluation in the following.

2.3.2 Precipitation statistics

For the compilation of precipitation statistics, it is common practice in Germany to carry out the procedure on the basis of DWA Worksheet 531 (Haberlandt et al., 2017). The methodology is applied for example in KOSTRA-DWD-2020 (Junghänel et al., 2022) and RADKLIM (Winterrath et al., 2017). It recommends the use of the Gumbel distribution (type I extreme value distribution) for annual series and the exponential distribution for partial series. The two parameters of the distribution function are adjusted separately for each duration and then balanced over defined duration ranges. The method provides stable estimates, especially for short time series up to 30 years, but are less suitable for statistical modeling of very extreme events at the edge of the distribution because of their lack of flexibility. In the context of flash floods, elimination of statistical outliers for a better fit of the distribution function is not really useful because they have a high information content about the extreme behavior of convective precipitation. It should be also mentioned that the statistical evaluation in DWA worksheet 531 was developed for the design of urban drainage systems using observation time series of 60 years and longer.

Fischer and Schumann (2018) developed an approach to extend the model to a three-parameter distribution function to better fit the statistics in the large precipitation event domain. The use of the generalized extreme value distribution (GEV) is recommended for an event duration less than 1 day (Bonnin et al., 2004), which is characterized by a variable shape parameter

https://doi.org/10.5194/egusphere-2023-1907
Preprint. Discussion started: 30 August 2023

ξ in addition to the location μ and scale parameter σ. The cumulative distribution function (CDF/ $F(x)$) and the quantile function ($F^{-1}(p)$)of the GEV are represented for $\xi \neq 0$ by Eq. 1 and 2:

$$F(x) = e^{-\left(1+\xi\cdot\left(\frac{x-\mu}{\sigma}\right)\right)^{-\frac{1}{\xi}}} \quad (1)$$

$$F^{-1}(p) = \mu - \frac{\sigma}{\xi}\cdot(1-(-\ln(p))^{-\xi}) \quad (2)$$

with x = random variables (precipitation depth) and p = probability (of undercutting). The Gumbel distribution is a special case of the GEV with ξ = 0 an is represented by Eq. 3 and 4:

$$F(x) = e^{-e^{-\left(\frac{x-\mu}{\sigma}\right)}} \quad (3)$$

$$F^{-1}(p) = \mu - \sigma\cdot\ln\cdot(-\ln(p)) \quad (4)$$

In the study of Fischer and Schumann (2018), the approach is examined on the basis of long station time series. The GEV model used can achieve better results than the DWA model, especially for duration steps between 45 min and 24 hours.

Both the DWA and GEV models are tested for estimating the annual extreme precipitation of the location-decoupled event series. In the first step, an estimate of the empirical recurrence intervals of the sample must be made. Based on this assignment, the parameters of the respective distribution function are then estimated in the next step. The plotting position formulas most commonly used in hydrology to show the empirical distribution are based on the general form given in Eq. 5 (Cunnane, 1978; Arnell et al. 1985):

$$p_i = \frac{i-\beta}{n+1-2\beta} \quad (5)$$

with n = sample size, i = rank (ascending) and β = fitting parameter for different distributions (varies from 0 to 0.5). In this study, the plotting position is chosen with the parameter β = 0.4 according to Cunnane (1978). The formula is used in the DWA model as well as for the GEV. The distribution parameters are estimated using the L-moment method recommended by Hosking (1990) or Bílková (2014). This provides robust results for small samples with statistical outliers (extreme values). The parameter estimation procedure is already described for flood statistics in DWA worksheet 552 (Blöschl et al., 2012) and put into context for the application of possible distribution functions.

2.3.3 Goodness of fit

The goodness of fit of the derived probability distribution is determined in this study both visually, by contrasting the CDF and the empirical distribution function (EDF) in a graph and by using appropriate non-parametric statistical tests for non-normally distributed data. The latter have the advantage of allowing an objective evaluation of the results. The Kolmogorov-Smirnov test (KS) and the Anderson-Darling test (AD) were chosen as traditional test statistics. In addition, a modified form of the Anderson-Darling test (MAD) is also used. The MAD test developed by Ahmad et al. (1988), proposes a differential calculation of goodness of fit for the upper and lower tails of a probability distribution. This makes the MAD particularly suitable for the application of the GEV model and for the observation of extreme values. Shin et al. (2012) have already applied and verified this method in a simulation experiment on precipitation data. To perform the test, the function values of the

https://doi.org/10.5194/egusphere-2023-1907
Preprint. Discussion started: 30 August 2023

empirical distribution $F_{EDF}(x_i)$ as well as the cumulative distribution $F_{CDF}(x_i)$ of all used models are needed in ascending order (i = 1, ..., n).

The KS goodness-of-fit test (one-sample test) checks whether a random variable follows a defined probability distribution. The test is applied in this study as the first level of rejection and is calculated and evaluated according to the following scheme:

$$D_{u,i} = |F_{EDF}(x_i) - F_{CDF}(x_i)| \quad (6)$$

$$D_{l,i} = |F_{EDF}(x_{i-1}) - F_{CDF}(x_i)| \quad (7)$$

$$D_{max} = \max(D_{u,i}, D_{l,i}) \quad (8)$$

$$D_{crit} = \frac{\sqrt{-0.5 \cdot \ln(\frac{\alpha}{2})}}{\sqrt{n}} \quad (9)$$

with $D_{u,i}/D_{l,i}$ = upper/lower difference, D_{max} = maximum difference, D_{crit} = critical value, i = rank (ascending). For the case $D_{max} > D_{crit}$, the null hypothesis is rejected.

The AD test applied in normal and modified form as the second and third rejection stages. The method is more sensitive to the distribution tails, moreover, in the modified form the upper distribution edge can be evaluated separately. The test statistic is defined as follows:

$$A_n^2 = -n - \sum_{i=1}^{n} \frac{2i-1}{n} \cdot [\ln(F_{CDF}(x_i)) + \ln(1 - F_{CDF}(x_{n-i+1}))] \quad (10)$$

with A_n^2 = AD test statistic, n = sample size, $F_{CDF}(x_i)$ = CDF for specified distribution (ascending). For the modified variant (MAD), Ahmad et al. (1988) define the following computing equations:

$$A_n^2 = AU_n^2 + AL_n^2 \quad (11)$$

with AU_n^2 = AD test statistic for upper Tail, AL_n^2 = AD test statistic for lower Tail.

$$AU_n^2 = \frac{n}{2} - 2 \cdot \sum_{i=1}^{n} \ln(F_{CDF}(x_i)) - \sum_{i=1}^{n} (2 - \frac{2i-1}{n}) \cdot \ln(1 - F_{CDF}(x_i)) \quad (12)$$

$$AL_n^2 = -\frac{3n}{2} + 2 \cdot \sum_{i=1}^{n} \ln(F_{CDF}(x_i)) - \sum_{i=1}^{n} \frac{2i-1}{n} \cdot \ln(F_{CDF}(x_i)) \quad (13)$$

In the case of the AD test, the critical values depend on the selected significance level and the distribution function. For the considered significance level of 5 %, critical values of A_{crit}^2= 0.757 (Stephens, 1977) for the whole AD statistics and nearly constant critical value $AU_{crit}^2 \approx 0.278$ (Ahmad et al., 1988; Shin et al., 2012) for the upper peak are reported in the literature. The same applies here: if $A_n^2 > A_{crit}^2$, the null hypothesis is rejected.

https://doi.org/10.5194/egusphere-2023-1907
Preprint. Discussion started: 30 August 2023

3 Data application and discussion of the results

The application of the methodology is based on the example of the German state of Hesse, as described in Sect. 2.1. The evaluation is performed for the entire study area with a boundary buffer of 1 km for both the 9 and 25 grid cell aggregation. The selected extent of extreme events is not only characteristic for convective precipitation events, but also representative for the influence range of flash floods in low mountain ranges in Hesse. The relevant precipitation durations are defined as 15, 30, 45, 60, 75 and 90 minutes. The results of the previous studies (Sect. 2.2) have shown that no sufficient number of extreme events can be identified for a duration greater than 90 minutes.

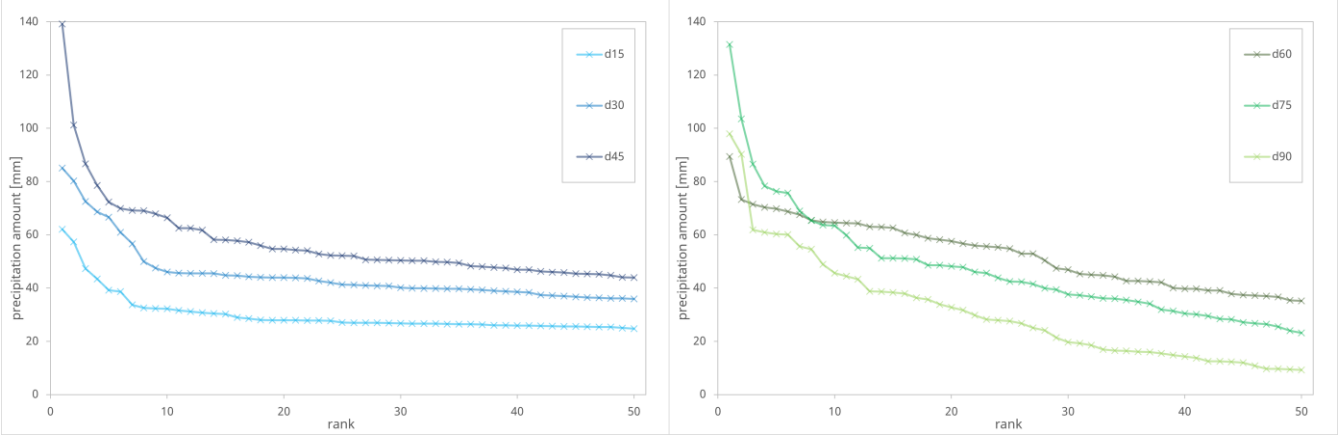

Figure 4: Comparison of the highest 50 precipitation depths (9 grid cell aggregation) in the event series for the 15 to 90 minutes durations.

The series of spatiotemporal independent extreme events (Perschke et al., 2023) resulting from the presented methodology (Sect. 2.3.1) are ordered by the absolute precipitation depth and plotted according to their rank. Figure 4 shows the first 50 ranks of the respective duration for the 9-pixel aggregation – the 25-pixel aggregation shows almost identical patterns of progression. For the durations up to 45 minutes (Fig. 4, left), events with larger precipitation depths are determined with increasing duration. In the range of the first 10 ranks, larger steps between the individual values and statistical outliers can be observed. With increasing rank, a slightly decreasing linear course is established. The higher durations of 60 minutes or longer (Fig. 4, right) show no increase in the overall level compared to the previous levels. It shows a contrary behavior. With an increase in the duration, the depth of precipitation decreases in proportion. Compared to the shorter durations, the graphs show a larger gradient and a lower total level. This extreme value behavior of convective events is a result of the unequivocal assignment of a characteristic duration. It supports the assumption that the most extreme manifestations of convective events take place in the range of less than 60 minutes. The classification into a higher duration would lead to an underestimation of the extreme behavior when evaluating the absolute depth of precipitation. It also shows that a longer event duration does not necessarily lead to higher precipitation totals.

Furthermore, the result of the event selection according to Sect. 2.3.1 provides information about the seasonal representativeness with respect to the study period and the precipitation intensity of the event series. Figure 5 shows the number

https://doi.org/10.5194/egusphere-2023-1907
Preprint. Discussion started: 30 August 2023

of independent events after applying the thresholds from table 2 (lighter bars) and the number after forming monthly block maxima (darker bars). As expected, the number of resulting events decreases with larger aggregation area and increasing duration. This leads to falling below the recommended minimum sample sizes of 2 times the number of observation years (Haberlandt et al., 2017) for a duration 75- and 90-minute – these are not considered in the further evaluation. The 60-minutes series is included in the further evaluation in spite of a low sample size and comparatively atypical behaviour. Despite the large data collectives of the durations smaller than 60 minutes – after applying POT method – there is no complete temporal coverage with 126 elements of the study period for any event series. It is necessary to check whether the event series are sufficiently representative in time and whether the interval of the block maxima is appropriate.

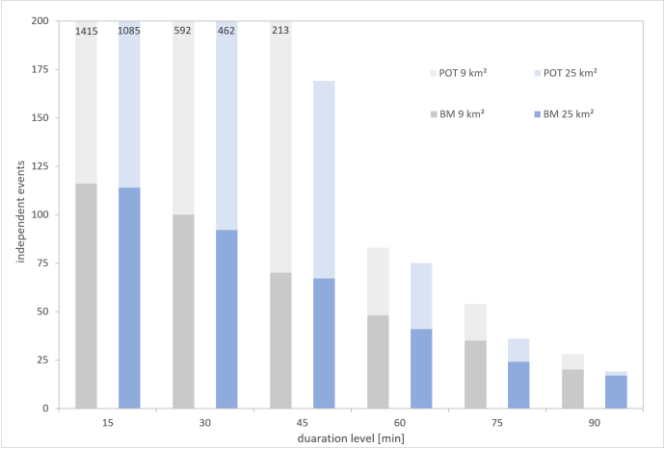

Figure 5: Selection of extreme events after using POT and BM method.

3.1 Temporal and spatial coverage

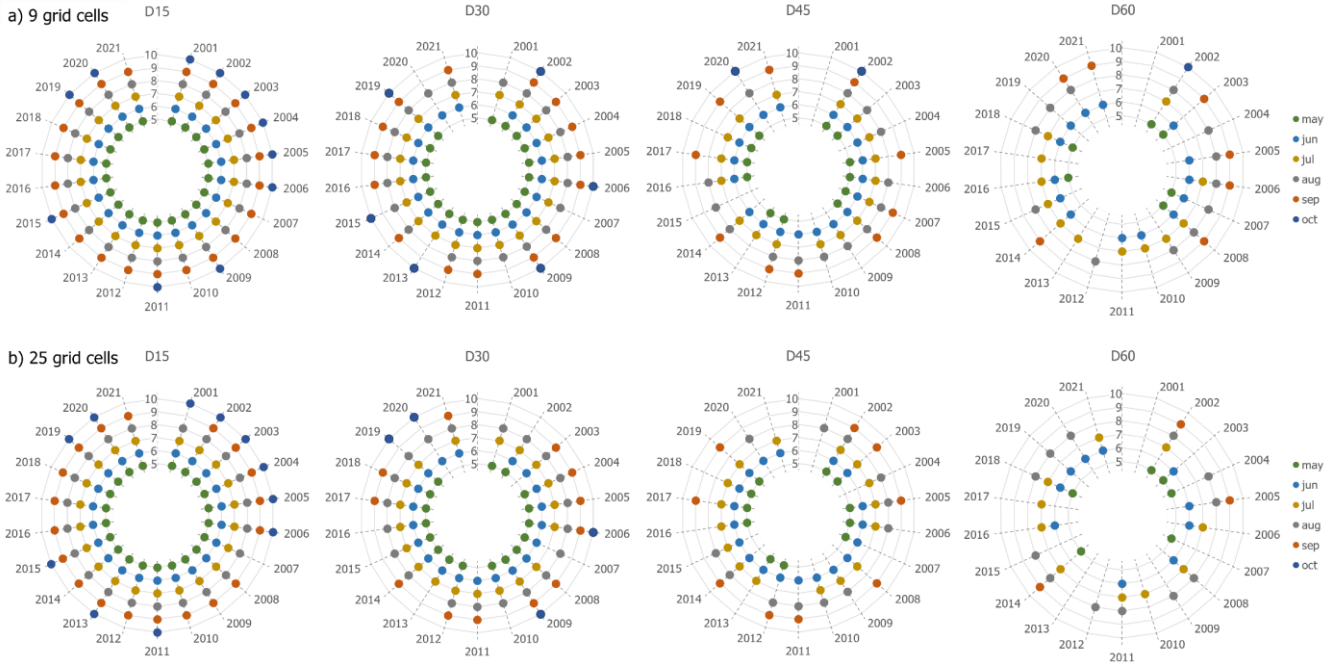

Figure 6: Monthly-differentiated temporal coverage of the observation period for the 15 to 60 minutes durations.

The next step is to take a more differentiated look at the temporal coverage of the study period. Figure 6 shows the time plotted event series of durations from 15 to 60 minutes for the 9 and 25 grid cell aggregation. For the 15-minute events, nearly complete

https://doi.org/10.5194/egusphere-2023-1907
Preprint. Discussion started: 30 August 2023

temporal coverage can be achieved for both extents. The 60-minute duration, conversely, exhibits a very scattered and patchy distribution, which can be attributed to the small sample size and the classification of the event duration. With increasing precipitation duration, the annual coverage decreases, especially in the late summer months of September and October. Robust coverage is noted for the peak summer months of June and July, as well as for the second half of May. Looking at the associated precipitation totals, there is no correlation of the maximum values with the month – excluding September and October – of occurrence. This evaluation shows that the most extreme convective events in Hesse occur from mid-May to late August. As a result, the sample can be assumed to be seasonally representative for the 45-minute and smaller durations.

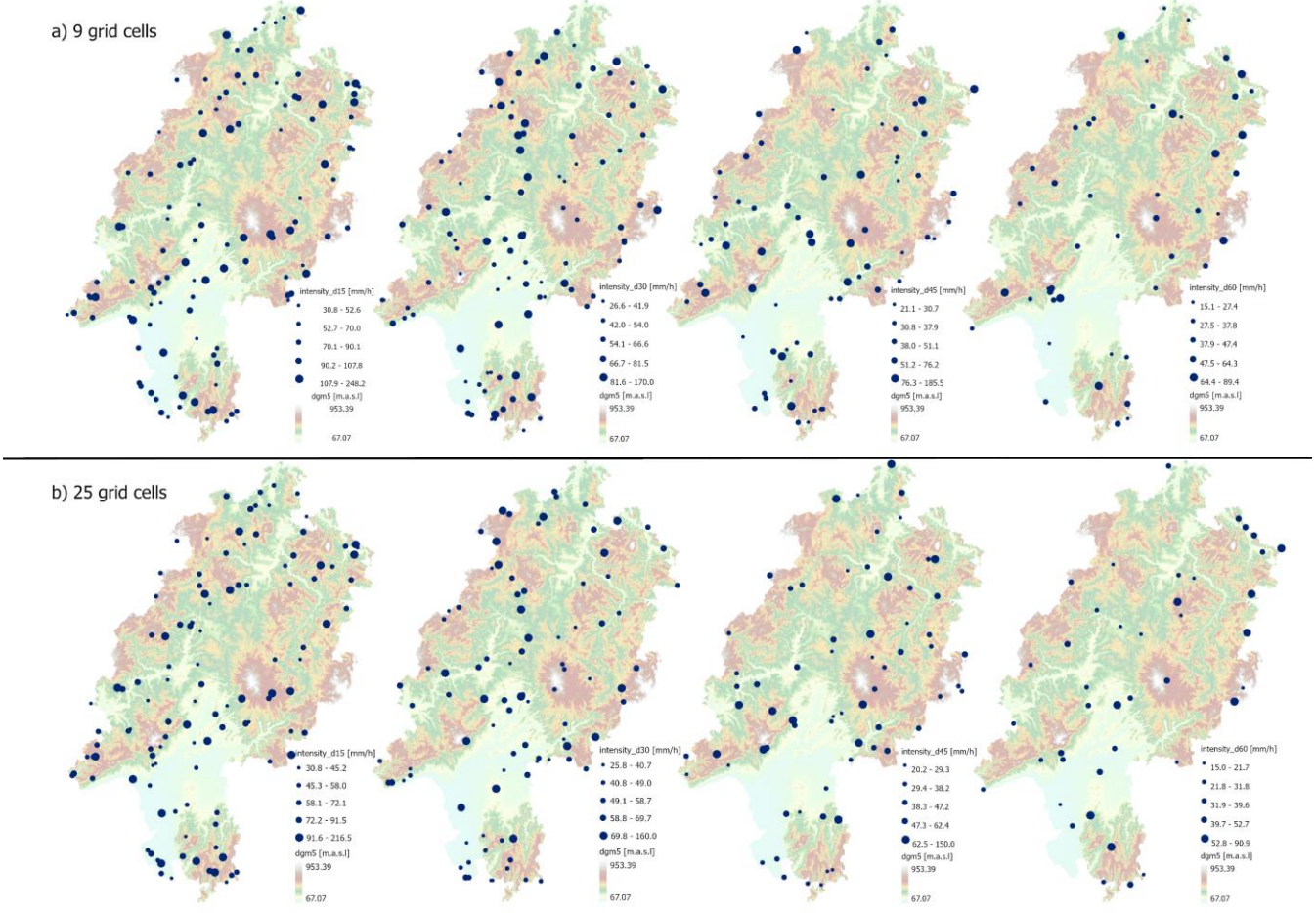

Figure 7: Spatial distribution and precipitation intensity of the selected extreme events for the 15 to 60 minutes durations. Base map: digital elevation model 5 [HVBG].

In the following, the spatial representativeness of the event series with consideration of the precipitation totals is examined and evaluated. Figure 7 shows the distribution of events in the study area differentiated by duration and extent. For a better evaluation of the orographic relation, the digital elevation model of Hesse is used as base map. The classification of the mean precipitation intensities of the individual events is based on the quintiles of the respective data collective. The maps show a

https://doi.org/10.5194/egusphere-2023-1907
Preprint. Discussion started: 30 August 2023

balanced and hotspot-free distribution of precipitation extremes for all durations. Upper quintile events are found at all elevations, confirming the assumption of orographic independence (Sect. 2.2.2) in the study area. In the lowlands, as well as in the area around the higher low mountain ranges, high intensity events are recorded. When overlaying the events of all durations, a relatively homogeneous spatial distribution results for both extents. Since no classification of events by their real extents is deliberately made, some events are identified in both aggregation levels. In addition to the temporal, the spatial representativeness of the event series can be confirmed up to the 45-minute events.

3.2 Application of the statistical models to the event series

In the final part of the evaluation, the statistical models described in Sect. 2.3.2 are applied to the event series. Taking into account the previous evaluation of the samples, further consideration is limited to the 15-, 30- and 45-minute durations. Figure 8 shows the results of the extreme value analysis separated for both aggregation levels. In the diagrams the quantile functions for GEV and Gumbel distribution are compared, for reference the plotting position of the sample elements is also shown. For the shape parameter ξ of the GEV – which significantly determines the skewness of the distribution – values between 0.02 and 0.17 are estimated. For $\xi > 0$ the GEV exhibits a heavy-tail behaviour. With respect to the predicted development of the convective potential in Central Europe, neglecting the heavy-tailed behaviour would lead to an underestimation of the recurrence interval at the upper distribution boundary (Merz et al., 2022). The Gumbel or the exponential distribution, on the other hand, show an exponential asymptotic (light tailed) behaviour. For the 15-minute events, there is only a slight difference in the quantiles between the two models.

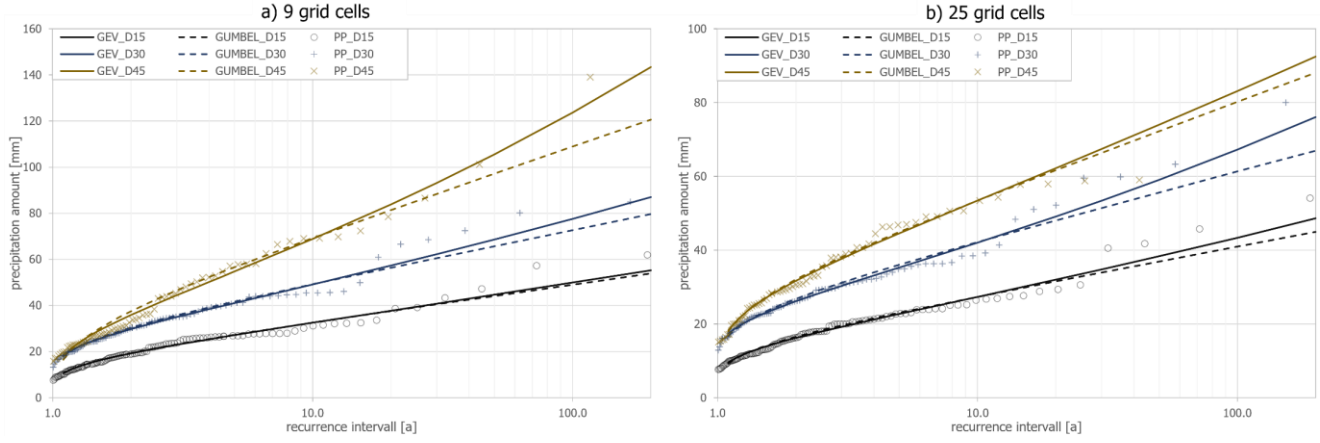

Figure 8: Comparison of the GEV and Gumbel distributions in relation to the plotting position (PP) for the 15-, 30- and 45-minutes samples.

For a more objective evaluation of the goodness of fit, selected statistical tests are performed as described in Sect. 2.3.3. The results of this evaluation can be found in Table 4, in all cases a significance level α of 5 % is used as decision criterion. Using the KS test, both the GEV and the Gumbel distribution can be accepted in all cases. The same result can be obtained for the AD test with the exception of the case D45_9_Gumbel – which has the highest value for ξ. The MAD test statistic shows a

https://doi.org/10.5194/egusphere-2023-1907
Preprint. Discussion started: 30 August 2023

higher rejection power on the side of the Gumbel distribution at a ξ value greater than 0.1, which is probably due to the heavy tail behaviour of the probability distribution. It can be stated that the GEV model has the better fitting performance when considering exceptional extreme events.

Table 4: Results of goodness-of-fit tests for the probability distributions fitted to the sample. Significance level α = 0.05 (note: KS is Kolmogorov-Smirnov statistic, A^2 is Anderson-Darling statistic and AU^2 is Modified-Anderson Darling statistic for the upper tail)

	GEV			Gumbel		
α = 0.05	KS	A^2	AU^2	KS	A^2	AU^2
D15_9	Accept	Accept	*Reject*	Accept	Accept	*Reject*
D30_9	Accept	Accept	Accept	Accept	Accept	Accept
D45_9	Accept	Accept	Accept	Accept	*Reject*	*Reject*
D15_25	Accept	Accept	Accept	Accept	Accept	Accept
D30_25	Accept	Accept	Accept	Accept	Accept	*Reject*
D45_25	Accept	Accept	Accept	Accept	Accept	Accept

3.3 Restrictions and Uncertainties

The presented method includes some strict assumptions that potentially limit its general application to other areas outside Central Europe. For the identification and classification of precipitation objects, fixed criteria - intensity threshold, rate of change of precipitation depth - are applied, which are assumed to be plausible for the considered sub-survey area over the whole area. A low orographic dependence in the observation area is widely assumed (cf. Sect. 2.2.2). It was not intended to conduct a spatial scaling analysis as part of this study yet. Thus, it remains to be seen whether comparable samples can be generated, especially for smaller sub-areas. The variability of the exceptional extreme events is crucial here. If too few exceptional or too many similar precipitation events are to be found in the upper ranks of the sample, the Gumbel model should be preferred. The applicability of the method as well as the plausibility and representativeness of the results can be guaranteed by the assumptions made and the scope defined.

With regard to the uncertainties, the methodology of the radar precipitation estimation should be pointed out first. With the use of time-normalized reanalysis data, as also in Reder et.al (2022) or Lengfeld et al (2023), a uniform reprocessing of the precipitation reflectivities can be ensured and some uncertainty factors can be eliminated. Furthermore, reference should be made at this point to the observation period under consideration, from 2001 to 2021. In addition to the discussed limited statistical significance of the period, the faster increasing climatic changes should also be pointed out here. The resulting uncertainties in the analysis of extreme precipitation can hardly be captured. The supposedly short observation period has the potential to give more weight to these momentary changes in the probability of occurrence of extreme events. In this context, the considered GEV model reacts flexibly to the increasingly extreme individual events in the upper ranks, which allows for their consideration in the statistics (Fischer and Schumann, 2018).

https://doi.org/10.5194/egusphere-2023-1907
Preprint. Discussion started: 30 August 2023

4 Conclusion

One big challenge in the analysis of heavy precipitation is the realistic identification and description as well as the statistical classification of convective extreme events. The specific characteristics of convective precipitation cells - small extent, short lifetime - require area-wide, spatial and temporally highly resolved precipitation data for representative coverage. From a climatological point of view, the german radar data used are only available for a short observation period (21 a). In local observation, this often leads to the fact that no sufficiently large sample of extreme events can be identified and also the combination with comparatively long time series of precipitation stations does not create a homogeneous data basis here. The low orographic dependence indicates that the strength of the events does not necessarily depend on the location of record, but rather on the state of the atmosphere respectively the precipitation cell. It is not decisive at which exact location the precipitation fell, but at which point in time the precipitation cell shows its most extreme form. The drift effects and sedimentation time of hydrometeors caused by the height of the radar detection are thus put into perspective.

With this study, a new approach of regionalized analysis of convective heavy precipitation is pursued in order to describe the extreme value behaviour. The focus is on the event and object view with respect to the specific duration and characteristic extent of the events. With the spatial aggregation, the precipitation sum of the events is averaged in an area effective size (9 and 25 km²) and thus scaled to a flash flood relevant catchment size of the low mountain ranges. This leads to a comprehensive catalog of locally decoupled, spatial and temporally independent events for the considered study area. In comparison to other methods (e. g. KOSTRA, RADKLIM), the events are categorized with respect to the course of the intensive main rainfall phase and assigned to an authoritative duration. It should be emphasized that the composition of the sample takes into account the temporal representativeness over the hydrological summer half-year. The results show a specific duration of 15 to 45 minutes for convective heavy precipitation events. In comparison, events with a duration of 60 minutes and longer are underrepresented either do not show a consistent extreme value behaviour. For the statistical classification regarding the probability of occurrence of the most extreme events, the GEV model is suitable, especially for the 30- and 45-minute events. For the shorter events, the recommended Gumbel model also shows a good fit. As the duration increases, the upper ranks show more extreme events, which have a strong effect on the shape of the distribution. Here, it would be widely necessary to examine how the change of the study area affects the results. By changing the scale of the study to the entire Central European low mountain sill and smaller sub-areas, the methodology can be further tested for its applicability and comparability. In any case, the orographic independence of convective heavy precipitation beyond Hesse should be ensured. This new approach proves to be promising in the context of this study and promotes the gain of knowledge in the context of the characterization of convective heavy precipitation. Based on this, it is possible to develop a radar-based new heavy rainfall model for use in flooding simulations and as dimensioning precipitation for protective measures.

https://doi.org/10.5194/egusphere-2023-1907
Preprint. Discussion started: 30 August 2023

Code and data availability. The generated data set 'Spatiotemporally independent heavy precipitation events for the state of Hesse (Germany)' can be retrieved at https://doi.org/10.5281/zenodo.8131633. The corresponding author (manuel.perschke@hs-rm.de) can provide access to any additional code and data created during this work upon request.

Competing interests. The contact author has declared that none of the authors has any competing interests.

Acknowledgements. The authors would like to acknowledge the German Weather Service for the provision of the radar precipitation data.

References

Ahmad, M.I., Sinclair, C.D., Spurr, B.D.: Assessment of flood frequency models using empirical distribution function statistics. Water Resour Res, 24(8), 1323–1328, https://doi.org/10.1029/WR024i008p01323, 1988.

Arnell, N.W., Beran, M., and Hosking, J.R.M.: Unbiased plotting positions for the general extreme value distribution, J. Hydro., 86, 59-69, https://doi.org/10.1016/0022-1694(86)90006-5, 1986.

Bednar-Friedl, B., Biesbroek, R., Schmidt, D.N., Alexander, P., Børsheim, K.Y., Carnicer, J., Georgopoulou, E., Haasnoot, M., Le Cozannet, G., Lionello, P., Lipka, O., Möllmann, C., Muccione, V., Mustonen, T., Piepenburg, D., and Whitmarsh, L.: Europe. In: Climate Change 2022: Impacts, Adaptation and Vulnerability, Contribution of Working Group II to the Sixth Assessment Report of the Intergovernmental Panel on Climate Change, Cambridge University Press, 1817–1927, https://doi.org/10.1017/9781009325844.015., 2022.

Berg, P., and J. O. Haerter: Unexpected increase in precipitation intensity with temperature—A result of mixing of precipitation types? Atmos. Res., 119, 56–61, https://doi.org/10.1016/j.atmosres.2011.05.012., 2013.

Bílková, D.: L-Moments and TL-Moments as an Alternative Tool of Statistical Data Analysis, J. appl. math. phys., 2, 919-929, http://doi.org/10.4236/jamp.2014.210104, 2014.

Blöschl, G., Büttner, U., Demuth, N., Holle, F., Meon, G., Merz, R., Müller, G., Schumann, A., and Barion, D.: Merkblatt DWA-M 552: Ermittlung von Hochwasserwahrscheinlichkeiten, Deutsche Vereinigung für Wasserwirtschaft, Abwasser und Abfall e. V., isbn: 978-3-942964-25-8, 2012.

Bonnin, G.M., Martin, D., Lin, B., Parzybok, T., Yekta, M., and Riley, D.: Precipitation-Frequency Atlas of the United States, National Oceanic and Atmospheric Administration (NOAA), Maryland, https://www.weather.gov/media/owp/oh/hdsc/docs/Atlas14_Volume2.pdf (last access: 31 July 2023), 2004.

Brendel, C., Brisson E. , Heyner F., Weigl E., and Ahrens B.: Bestimmung des atmosphärischen Konvektionspotentials über Thüringen, Berichte des Deutschen Wetterdienstes Nr. 244, Offenbach am Main, https://publikationen.ub.uni-frankfurt.de/opus4/frontdoor/deliver/index/docId/42315/file/DWD_Berichte_244_Druckvorlage_(low).pdf (last access: 31 July 2023), 2014.

Cunnane, C.: Unbiased plotting positions – a review, J. Hydro., 37(3): 205-222, 1978.

Fischer, S., and Schumann, A.: Berücksichtigung von Starkregen in der Niederschlagsstatistik, HyWa, 62(4), 248-256, http://doi.org/10.5675/HyWa_2018,4_2, 2018.

Haberlandt, U., Kuchenbecker, A., Malitz, G., Miegel, K., Pfister, A., Prellberg, D., Sympher, K.-J., Verworn, H.-R., Winkler, U., Draschoff, R., and Stalmann, V.: Arbeitsblatt DWA-A 531. Starkregen in Abhängigkeit von Wiederkehrzeit und Dauer. korrigierte Fassung, Deutsche Vereinigung für Wasserwirtschaft, Abwasser und Abfall e. V., isbn: 978-3-942964-28-9, 2017.

Hosking, J.R.M.: L-Moments: Analysis and Estimation of Distributions Using Linear Combinations of Order Statistics. J. R. Stat. Soc., B, 52, 105-124, 1990.

https://doi.org/10.5194/egusphere-2023-1907
Preprint. Discussion started: 30 August 2023

Junghänel, T., Bär, F., Deutschländer, T., Haberlandt, U., Otte, I., Shehu, B., Stockel, H., Stricker, K., Thiele, L.-B., and Willems, W.: Methodische Untersuchungen zur Novellierung der Starkregenstatistik für Deutschland (MUNSTAR). Synthesebericht, https://www.dwd.de/DE/leistungen/kostra_dwd_rasterwerte/download/Synthesebericht_MUNSTAR_pdf.pdf?__blob=publicationFile&v=3#:~:text=Das%20Forschungsprojekt%20„Methodische%20Untersuchungen%20zur,aktueller%20Daten%20umfassend%20zu%20testen. (last access: 31 July 2023), 2022.

Kirshbaum, D. J., Adler, B., Kalthoff, N., Barthlott, C., and Serafin. S.: Moist Orographic Convection: Physical Mechanisms and Links to Surface-Exchange Processes, Atmos., 9, no. 3:80, http://doi.org/10.3390/atmos9030080, 2018.

Knist, S., Goergen, K., and Simmer, C.: Evaluation and projected changes of precipitation statistics in convection-permitting WRF climate simulations over Central Europe, Clim Dyn 55, 325–341, https://doi.org/10.1007/s00382-018-4147-x, 2020.

Kreklow, J., Tetzlaff, B., Kuhnt, G., and Burkhard, B.: A Rainfall Data Intercomparison Dataset of RADKLIM, RADOLAN, and Rain Gauge Data for Germany. Data, 4, 118. https://doi.org/10.3390/data4030118, 2019.

Lenderink, G., Barbero, R., Loriaux, J.M., and Fowler, H.J.: Super-Clausius–Clapeyron scaling of extreme hourly convective precipitation and its relation to large-scale atmospheric conditions, J. Climatol., 30, 6037–6052, https://doi.org/10.1175/JCLI-D-16-0808.1, 2017.

Lengfeld, K., Walawender, E., Winterrath, T., Weigl, E., and Becker, A Heavy precipitation events Version 2022.01 exceeding return period of 5 years based on RADKLIM-RW Version 2017.002, Parameter and polygons of heavy precipitation events in Germany. Version v2022.01, Deutscher Wetterdienst (DWD) [data set], http://doi.org/10.5676/DWD/CatRaRE_T5_Eta_v2022.01, 2022.

Lengfeld, K., Voit, P., Kaspar, F., and Heistermann, M.: Brief communication: On the extremeness of the July 2021 precipitation event in western Germany, Nat. Hazards Earth Syst. Sci., 23, 1227–1232, https://doi.org/10.5194/nhess-23-1227-2023, 2023.

Merz, B., Basso, S., Fischer, S., Lun, D., Bloschl, G., Merz, R., et al.: Understanding heavy tails of flood peak distributions. Water Resour. Res., 58, https://doi.org/10.1029/2021WR030506, 2022.

Müller, C., Nied, M., Voigt, M., Iber, C., Sauer, T., Junghänel, T., Hoy. A., and Hübener, H.: Starkniederschläge Entwicklungen in Vergangenheit und Zukunft, Klimaveränderung und Konsequenzen für die Wasserwirtschaft (KLIWA), https://www.kliwa.de/_download/KLIWA-Kurzbericht_Starkregen.pdf (last access: 31 Juli 2023), 2019.

Perschke, M., Schmalz, B., Ruiz Rodriguez, E.: Spatiotemporally independent heavy precipitation events for the state of Hesse (Germany), RheinMain University od Applied Science [data set], https://doi.org/10.5281/zenodo.8131633, 2023.

Purr, C., Brisson, E., and Ahrens, B.: Abschlussbericht zum Projekt: Konvektive Gefährdung über Hessen und Rheinland-Pfalz, Goethe-Universität Frankfurt am Main, Frankfurt am Main, https://www.klimawandel-rlp.de/fileadmin/website/klimakompetenzzentrum/downloads/Projekte/181207EndberichtAhrensKonv.pdf (last access: 31 July 2023), 2018.

Purr, C., Brisson, E., and Ahrens, B.: Convective rain cell characteristics and scaling in climate projections for Germany, Int. J. Climatol., 41, 3174– 3185, https://doi.org/10.1002/joc.7012, 2021.

Reder, A., Raffa, M., Pandulao, R., Rianna, G., Mercogliano, P.: Characterizing extreme values of precipitation at very high resolution: An experiment over twenty European cities, Weather Clim. Extrem, 35, https://doi.org/10.1016/j.wace.2022.100407, 2022.

Shin, H., Jung, Y., Jeong, C. et al.: Assessment of modified Anderson–Darling test statistics for the generalized extreme value and generalized logistic distributions, Stoch. Environ. Res. Risk. Assess., 26, 105–114, https://doi.org/10.1007/s00477-011-0463-y, 2012.

Stephens, M. A.: Goodness of Fit for the Extreme Value Distribution, Biometrika, 64(3), 583–588, https://doi.org/10.2307/2345336, 1977.

Winterrath, T., Brendel, C., Hafer, M., Junghänel, T., Klameth, A., Walawender, E., Weigl, E., and Becker, A.: Erstellung einer radargestützten Niederschlagsklimatologie, Berichte des Deutschen Wetterdienstes Nr. 251, Deutscher Wetterdienst, Offenbach am Main, https://www.dwd.de/DE/leistungen/pbfb_verlag_berichte/ pdf_einzelbaende/251_pdf.pdf?__blob=publicationFile&v=2 (last access: 31 July 2023), 2017.

https://doi.org/10.5194/egusphere-2023-1907
Preprint. Discussion started: 30 August 2023

Winterrath, T., Brendel, C., Hafer, M., Junghänel, T., Klameth, A., Lengfeld, K.,Walawender, E.,Weigl, E., and Becker, A.: Gaugeadjusted one-hour precipitation sum (RW), RADKLIM Version 2017.002: Reprocessed gauge-adjusted radar data, one-hour precipitation sums (RW), Deutscher Wetterdienst (DWD) [data set], https://doi.org/10.5676/DWD/RADKLIM_RW_V2017.002, 2018.